Int. J. Corros. Scale Inhib., 2024, **13**, no. 2, 1164–1185

1164

Understanding the impact of inhibitor concentration, immersion periods, and temperature on the corrosion inhibition of 2-piperazin-1-yl-1,3-benzothiazole in HCl solution

B.S. Mahdi,[1] H.M. Habeeb,[2] I.A.A. Aziz,[1] M.M. Hanoon,[1] F.F. Sayyid,[1] A.M. Mustafa,[1] T.S. Gaaz,[3] A.H. Jaaz,[4] A.A. Khadom,[5] E. Yousif[6] and A. Alamiery[7,8]*

[1]*Production and Metallurgy Engineering Department, University of Technology-Iraq, P.O. Box: 10001, Baghdad, Iraq*
[2]*College of Engineering, Department of Materials Engineering, University of Kufa, P.O. Box: 54002, Kufa, Najaf, Iraq*
[3]*Air Conditioning and Refrigeration Techniques Engineering Department, College of Engineering and Technologies, Al-Mustaqbal University, Babylon 51001 Iraq*
[4]*Medical Physics Department, College of Science, Al-Mustaqbal University, Babylon 51001 Iraq*
[5]*Department of Chemical Engineering, College of Engineering, University of Diyala, Diyala 32008, Iraq*
[6]*Department of Chemistry, College of Science, Al-Nahrain University, Baghdad 10001, Iraq*
[7]*Energy and Renewable Energies Technology Center, University of Technology, Iraq, P.O. Box: 10001, Baghdad, Iraq*
[8]*Department of Chemical and Process Engineering, Faculty of Engineering and Build Environment, Universiti Kebangsaan Malaysia, P.O. Box: 43600, Bangi, Selangor, Malaysia*
*E-mail: dr.ahmed1975@gmail.com

Abstract

The corrosion inhibition potential of 2-piperazin-1-yl-1,3-benzothiazole (PYB) for mild steel in 1.0 M hydrochloric acid (HCl) was comprehensively investigated through weight loss measurements and quantum chemical calculations. The study delved into the influence of various corrosion inhibition parameters, including PYB concentration, immersion times, and temperature. Remarkably, the highest inhibition efficiency of PYB reached 90.7% at a concentration of 0.5 mM and a temperature of 303 K. Notably, inhibition efficiency demonstrated an upward trend with increasing concentration. Weight loss techniques affirmed that inhibition efficiency correspondingly increased with prolonged immersion times, as well as with elevated temperature. Furthermore, the observed higher inhibition performance with increasing temperature was corroborated by the calculated $\Delta G°$ values, suggesting that PYB actively participates in both physical and chemical adsorption processes on the mild steel surface. The adsorption phenomenon adhered to the Langmuir adsorption isotherm, as

supported by experimental and theoretical findings, which exhibited commendable agreement. This study presents a comprehensive understanding of the corrosion inhibition mechanism of PYB, offering valuable insights for future applications in corrosion mitigation strategies.

1. Introduction

Corrosion inhibition is a crucial area of research extensively considered and studied due to its effectiveness in protecting materials against degradation, offering a cost-effective and efficient solution [1, 2]. Mild steel, a common material used in various industrial applications, is particularly susceptible to corrosion in acidic environments. Acids are widely employed in industrial processes, making corrosion inhibition strategies imperative for maintaining material integrity and prolonging service life. Corrosion inhibitors can be categorized as organic or inorganic compounds. Inorganic inhibitors, such as chromates and phosphates, offer advantages such as high temperature stability and robust protection against corrosion [3, 4]. However, they often pose environmental and health hazards, limiting their widespread use [5]. Organic inhibitors, on the other hand, provide environmentally friendly alternatives with high efficiency and versatility. Nonetheless, their performance may vary depending on factors such as chemical structure and environmental conditions [6–10]. The research community has witnessed significant interest in the development of effective organic inhibitors containing heteroatoms (such as oxygen, nitrogen, and sulfur) and functional groups like triple bonds, conjugated double bonds, or aromatic rings in their molecular structures. One such compound of interest is 2-piperazin-1-yl-1,3-benzothiazole (PYB), a sulfur- and nitrogen-containing compound. PYB's ability to interact with metals through its heteroatoms, which readily react with d-orbitals of metals, renders it a promising corrosion inhibitor candidate. However, the complexity of its molecular structure may influence its corrosion inhibition ability and necessitates further investigation.

In 2022, a study investigated the corrosion inhibition of mild steel in hydrochloric acid using piperazine derivatives. The study focused on the corrosion inhibition performance of 1,4-bis(2-(2-hydroxyethyliminomethyl)phenyl)piperazine on carbon steel in 1.0 M HCl solutions, demonstrating its effectiveness as a corrosion inhibitor [11]. Another study in 2022 examined the corrosion mitigation performance of bis-benzothiazole derivatives for mild steel in aqueous 1 M HCl. The study provided insights into the corrosion inhibition efficiency of the bis-benzothiazole derivatives, highlighting their potential as effective corrosion inhibitors for mild steel in HCl solutions [12]. The results revealed that the synthesized piperazine derivatives exhibited excellent performance as corrosion inhibitors for mild steel in 1 M HCl solution [13]. A literature review in 2013

discussed the use of benzothiazole derivatives as corrosion inhibitors for steel in HCl solutions. The review highlighted the inhibitive effects of benzothiazole derivatives on mild steel corrosion, emphasizing their potential as corrosion inhibitors in acidic environments [14]. In 2023, a new benzisoxazole derivative was studied as a potential corrosion inhibitor for mild steel in 0.5 M hydrochloric acid medium. The investigation provided insights into the corrosion inhibition efficiency of the benzisoxazole derivative, demonstrating its potential as a corrosion inhibitor for mild steel in HCl solutions [15]. Furthermore, in 2023, the corrosion inhibition of mild steel in 1 M hydrochloric acid solutions by new *N,N'*-bipyrazole piperazine derivatives was investigated. The study demonstrated the potential of the synthesized piperazine derivatives as effective corrosion inhibitors for mild steel in HCl solutions [16]. These studies collectively underscore the potential of both piperazine derivatives and benzothiazole derivatives as effective corrosion inhibitors for mild steel in HCl solutions, offering valuable insights into their corrosion inhibition performance. Herein, the investigated compound PYB possesses both piperazine and benzothiazole functionalities, thus combining the corrosion inhibition properties of both groups synergistically.

Despite the considerable body of research on corrosion inhibitors, there remains a need to explore novel compounds and understand their mechanisms of action. Several studies have reported the effectiveness of various corrosion inhibitors, shedding light on their potential applications and optimization strategies. The objective of this study is to investigate the corrosion inhibition ability of 2-piperazin-1-yl-1,3-benzothiazole (PYB) as in Figure 1, for mild steel in HCl solution. The aim is to assess the influence of PYB concentration, immersion times, and temperature on corrosion inhibition effectiveness through weight loss measurements and quantum chemical calculations. This research contributes to the understanding of PYB's corrosion inhibition mechanism and its potential application as a protective agent for mild steel in acidic environments. By combining experimental and theoretical approaches, novel insights into the influence of key parameters on corrosion inhibition performance are elucidated. Additionally, the study investigates the adsorption behavior of PYB on the metal surface, providing valuable information for the development of effective corrosion mitigation strategies.
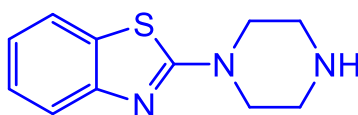
Figure 1. The chemical structure of PYB.

2. Materials and Methods

Mild steel coupons, obtained from the Company of Metal Samples, served as the working electrodes for this investigation. The chemical composition of the mild steel, expressed in weight percentage, is detailed in Table 1. Standard cleaning procedures outlined in method G1-03/ASTM [17] were employed to prepare the mild steel coupons.

Table 1. Chemical composition of mild steel coupon (wt.%).

Carbon	Manganese	Silicon	Aluminum	Sulfur	Phosphorus	Iron
0.210	0.050	0.380	0.010	0.050	0.090	balance

2.1. Acidic solution

The acidic solution utilized in the investigations was a 1 M hydrochloric acid solution, prepared by diluting analytical reagent-grade HCl (37%) with double-distilled water.

2.2. Weight loss investigations

Weight loss analyses were conducted in an environment of 1 M HCl, both in the absence and presence of the tested corrosion inhibitor, on mild steel coupons measuring $45 \times 25 \times 0.2$ mm. Prior to testing, the coupons were meticulously sanded with various grades of sandpaper up to 1200 grits. Each test was performed in a 250 mL beaker containing 100 mL of 1 M HCl solution as the corrosive medium. Clean coupons were initially weighed and then immersed in the corrosive solution. After exposure periods of 1, 5, 10, 24 and 48 hours, the coupons were removed, rinsed with double-distilled water, cleaned with acetone, dried in an oven, and reweighed using an electronic balance. Corrosion rate (*CR*; mm/y) and inhibition efficiency (*IE*%) were calculated from weight loss measurements based on Equations 1 and 2 respectively [18–20]:

$$C_{\mathrm{R}} = \frac{8.76(W_{\mathrm{initial}} - W_{\mathrm{final}})}{At} \tag{1}$$

$$C_{\mathrm{R}} = \frac{8.76(W_{\mathrm{initial}} - W_{\mathrm{final}})}{At} \cdot 100 \tag{2}$$

The reproducibility of the weight-loss test was ensured by conducting multiple trials under controlled conditions and calculating the average corrosion rate.

2.3. Effect of temperature

Temperature-dependent investigations were conducted at 303 K, 313 K, 323 K, and 333 K using mild steel coupons of chosen thickness. Similar to the weight loss investigations, each test was conducted in a 250 mL beaker with 100 mL of 1 M HCl solution as the corrosive environment. Following a 5-hour exposure period, coupons were removed, cleaned, and weighed as described above. All experiments were repeated three times [20].

2.4. Adsorption isotherms

Understanding the adsorption behavior of the tested compounds provides crucial insights into their characteristics. The degree of surface coverage (θ) by inhibitors can be elucidated through the application of various adsorption isotherms, including Langmuir, Freundlich,

and Temkin. In this study, weight loss measurements were conducted to determine the surface coverage values (θ) for different inhibitor concentrations in acidic media, utilizing a scale with a sensitivity of 0.001 g [21].

$$\text{Langmuir Isotherm Equation: } \frac{C}{\theta} = \frac{1}{K_{ads}} + C \tag{3}$$

$$\text{Temkin Isotherm Equation: } \theta = \frac{-\ln K_{ads}}{2a} - \frac{\ln C}{2a} \tag{4}$$

$$\text{Frumkin Isotherm Equation: } \ln \frac{\theta}{1-\theta} = \ln K_{ads} + 2a \tag{5}$$

where θ represents the degree of surface coverage, C denotes the concentration, and K_{ads} signifies the equilibrium adsorption constant.

2.5. Computational Details

Ground-state geometries were computed using Gaussian 03, Revision C.01, optimized to a local minimum without symmetry restrictions employing the valence and polarization basis set (6-31G^{++}(d,p)). Gas-phase calculations were performed using the B3LYP (Becke three-parameter hybrid exchange functional combined with Lee–Yang–Parr correlation functional) density functional theory (DFT) method to determine optimized geometries, HOMO energies (E_{HOMO}), LUMO energies (E_{LUMO}), and relevant physical properties for the molecules under study. HOMO, LUMO, ΔE, η, σ, χ, and ΔN were calculated using Equations 6–10, where χ_{Fe} and η_{Fe} represented 7 eV/mol and 0 eV/mol, respectively [22–25].

$$\Delta E = E_{HOMO} - E_{LUMO} \tag{6}$$

$$\eta = -\left(E_{HOMO} - E_{LUMO}\right)/2 \tag{7}$$

$$\sigma = 1/\eta \tag{8}$$

$$\chi = -(E_{HOMO} + E_{LUMO})/2 \tag{9}$$

$$\Delta N = (\chi_{Fe} - \chi_{inh})/2(\eta_{Fe} - \eta_{inh}) \tag{10}$$

3. Results and Discussion

3.1. Gravimetrical measurements

3.1.1. Effect of concentration

The investigation into the effect of PYB concentration on corrosion inhibition revealed a clear trend: as the concentration of PYB increased, the anticorrosion performance improved. Specifically, at a temperature of 303 K and a five-hour exposure period, the

corrosion rate exhibited a noticeable decrease with increasing PYB concentration. The highest inhibitory efficiency, reaching 90.7%, was attained at a concentration of 0.5 mM PYB (Figure 2). The observed enhancement in corrosion inhibition performance with increasing PYB concentration can be attributed to several factors rooted in its molecular structure. The presence of aromatic groups in PYB increases the electron density at active sites, facilitating stronger interactions between PYB molecules and iron atoms on the metallic substrate. Additionally, the nitrogen and sulfur atoms within the PYB structure form coordination bonds with the metal surface, further enhancing the adsorption of PYB and promoting the formation of a protective layer against corrosion. However, it is important to note that the effect of different concentrations of corrosion inhibitors on mild steel in 1 M HCl solution can vary. While higher concentrations generally lead to better corrosion protection, the optimal concentration may depend on factors such as the specific inhibitor, temperature, and the presence of other ions in the solution [26, 27]. Moreover, some inhibitors may exhibit diminished effectiveness or even become corrosive themselves at high concentrations. In the weight loss tests conducted on metallic coupons in both inhibited and uninhibited corrosive solutions, the presence of PYB, acting as a corrosion inhibitor, effectively shielded the metallic surface from the corrosive solution. Overall, the molecular structure and chemical composition of PYB play pivotal roles in its corrosion inhibition ability. The heterogeneous atoms and functional groups present, particularly the aromatic groups, facilitate strong interactions with the metal surface, rendering PYB an effective corrosion inhibitor. The adsorption of PYB molecules onto the surface of mild steel coupons results in the formation of a protective film, which becomes more pronounced with increasing PYB concentration up to 0.5 mM. Beyond this concentration, the inhibitory efficiency remains relatively constant, as the protective film acts as a barrier to corrosive agents and neutralizes them, thereby reducing the corrosion rate.

Various studies have explored the impact of different inhibitor concentrations on mild steel corrosion rates in acidic solutions. For example, Fang investigated several organic corrosion inhibitors in 1 M HCl solution and found that higher inhibitor concentrations generally led to lower corrosion rates, albeit with variations depending on the inhibitor type. Similarly, studies on the influence of natural inhibitors, such as pomegranate peel extract and castor oil, have shown concentration-dependent corrosion rate reduction, with optimal concentrations yielding peak inhibition efficiency [29, 30]. In conclusion, PYB molecules exhibit significant potential as corrosion inhibitors in acidic environments, effectively reducing corrosion rates and safeguarding metal surfaces through the formation of a stable and protective film. The optimal concentration of PYB for achieving maximum inhibitory efficiency is determined to be 0.5 mM, beyond which further increases have minimal impact on inhibition efficiency.
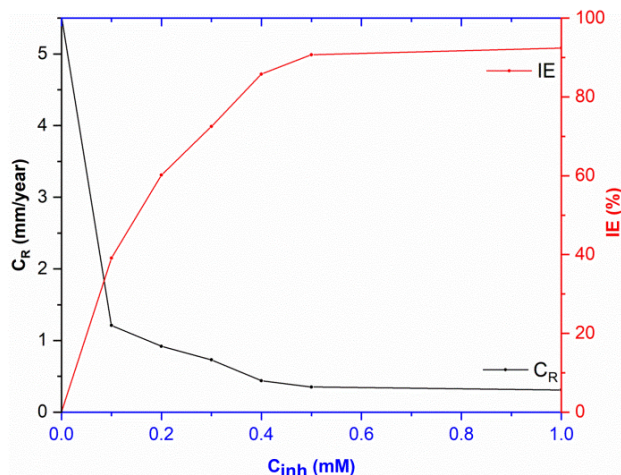
Figure 2. The corrosion rate and inhibition efficiency of mild steel exposed to a 1 M HCl solution for 5 hours at 303 K, examined across various concentrations of PYB.

3.1.2. Effect of immersion periods

To assess the impact of immersion periods on the efficacy of PYB in corrosion reduction/prevention, mild steel samples were subjected to 1 M HCl solutions with varying concentrations of PYB (ranging from 0.1 to 1.0 mM) for different immersion durations (1 hour to 48 hours) at 303 K (Figure 3).
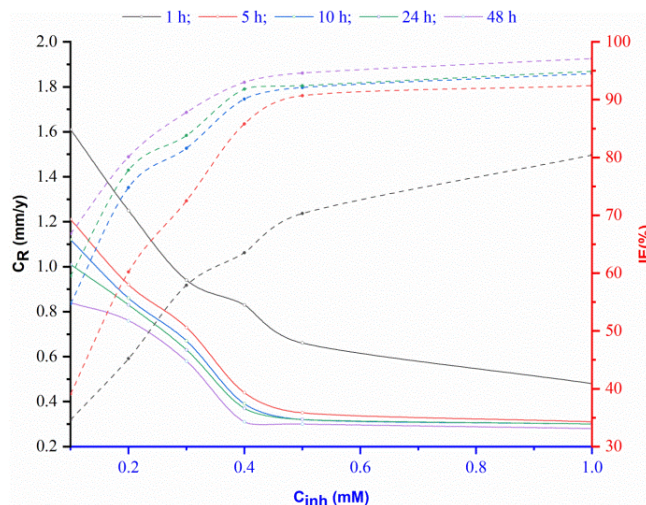
Figure 3. Effect of PYB concentration on corrosion rate and inhibition efficiency of metallic coupons in 1 M HCl for various immersion periods at 303 K.

The results revealed a substantial decrease in corrosion rate with increasing concentrations of PYB. Notably, at 0.1 mM PYB, the corrosion rate was notably high (1.21 mm/y), whereas at 0.5 mM, it decreased to 0.35 mm/y, reaching its lowest point (0.31 mm/y) at 1.0 mM PYB, marking a nearly 74% reduction compared to the 0.1 mM concentration [31, 32]. Furthermore, immersion time significantly influenced PYB's effectiveness in corrosion reduction. Prolonged immersion durations corresponded to

enhanced corrosion reduction efficacy. For instance, at 1.0 mM PYB, the lowest corrosion rate was observed after 48 hours of immersion (0.28 mm/y), showcasing a 30% decrease compared to the one-hour immersion period (0.48 mm/y). In conclusion, immersion periods exert a notable effect on PYB's efficacy in corrosion reduction. Higher concentrations of PYB and longer immersion durations proved more effective in reducing corrosion, suggesting PYB's potential as an alternative to conventional corrosion inhibitors for metal surface protection. The inhibitory efficiency of PYB on metal substrates demonstrated rapid enhancement with increasing immersion periods, peaking between 10 to 48 hours. This enhancement is attributed to the heightened adsorption of PYB molecules onto the metal substrate, facilitated by the catalytic effect of the metal surface. The resultant uniform coating of PYB molecules acts as a barrier against corrosion, bolstering inhibitory efficiency [33, 34]. The complex inhibitory process of PYB is influenced by various factors including temperature, pH, and solution concentration, all of which must be carefully managed for optimal efficacy. Notably, strong hydrogen bonding and coordination interactions between PYB molecules and the metal substrate contribute to its stability and effectiveness as a corrosion inhibitor in acidic environments. The high adsorption density of PYB enables both physisorption and chemisorption, further reinforcing its protective layer and enhancing inhibitory efficacy [35]. The sustained inhibitory efficacy of PYB over prolonged exposure periods underscores its potential as a corrosion inhibitor, offering prolonged protection against corrosive agents and highlighting its utility in metal surface preservation.

3.1.3. Effect of temperature

Temperature plays a critical role in influencing the interaction between the mild steel surface and the corrosive environment, both in the absence and presence of a tested inhibitor such as PYB. The impact of temperature on corrosion rate and protection efficiency was investigated through weight loss measurements conducted on mild steel samples immersed in 1 M HCl solution, supplemented with various concentrations of PYB, across the temperature range of 303–333 K (Figure 4). The weight loss data revealed a consistent trend: as temperature increased, the corrosion rate exhibited a noticeable decrease in the presence of various inhibitor concentrations over a 5-hour immersion period [36, 37]. This phenomenon suggests that higher temperatures contribute to a reduction in the corrosive activity on the mild steel surface, particularly in the presence of PYB molecules.

Furthermore, the surface coverage (θ), determined by the ratio of inhibition efficiency (*IE*) to 100, showed a slight increase with rising temperature in the presence of PYB. This observation suggests that at elevated temperatures, there is enhanced adsorption of PYB molecules onto the mild steel surface. However, the marginal increase in surface coverage implies that the protective performance of PYB is largely unaffected by temperature variations within the investigated range [38, 39]. To illustrate, consider the following scenario: at a temperature of 303 K, the corrosion rate in the presence of PYB may be

measured at 0.5 mm/year, whereas at 333 K, it decreases to 0.3 mm/year. This reduction in corrosion rate with increasing temperature indicates the beneficial effect of elevated temperatures on corrosion inhibition, attributed to the enhanced adsorption and protective properties of PYB molecules [40]. Overall, the findings suggest that PYB functions as an effective inhibitor across the temperature range investigated, with its protective performance remaining largely independent of temperature fluctuations. This temperature stability makes PYB a reliable corrosion inhibitor under varying environmental conditions, enhancing its potential for practical applications in corrosion protection strategies for mild steel. However, further investigations may be warranted to explore the specific mechanisms underlying the temperature dependence of corrosion inhibition and its implications for real-world scenarios.

The observed decrease in the corrosion rate of mild steel with an increase in temperature, as depicted in Figure 4, can be attributed to various underlying factors, encompassing alterations in reaction kinetics and the thermodynamics governing the corrosion process.

Firstly, it is well-established that temperature exerts a significant influence on reaction kinetics. At higher temperatures, the rates of chemical reactions typically accelerate due to the heightened kinetic energy of the reacting molecules. In the context of corrosion inhibition, this increased kinetic energy facilitates more rapid inhibitor adsorption onto the metal surface. Consequently, a greater number of inhibitor molecules are able to attach themselves to the metal, forming a denser and more protective layer that acts as a barrier against corrosive agents. Moreover, the thermodynamics of the corrosion process are also influenced by temperature variations. Generally, higher temperatures promote the dissolution of chemical species and the diffusion of reactants, which can affect the overall corrosion rate. In the presence of corrosion inhibitors such as PYB, elevated temperatures may enhance the thermodynamic favorability of inhibitor adsorption onto the metal surface. This thermodynamic favorability, coupled with the accelerated reaction kinetics, results in a more effective inhibition of corrosion at higher temperatures. Furthermore, it is important to consider the effect of temperature on the stability and reactivity of the corrosion products formed on the metal surface. At elevated temperatures, the structure and composition of these corrosion products may undergo changes, potentially leading to alterations in their protective properties. This, in turn, can influence the overall corrosion rate of the metal. In summary, the decrease in the corrosion rate of mild steel with an increase in temperature can be attributed to the combined effects of enhanced reaction kinetics and favorable thermodynamics for inhibitor adsorption. These factors contribute to the formation of a more protective inhibitor layer on the metal surface, thereby mitigating the corrosion process.
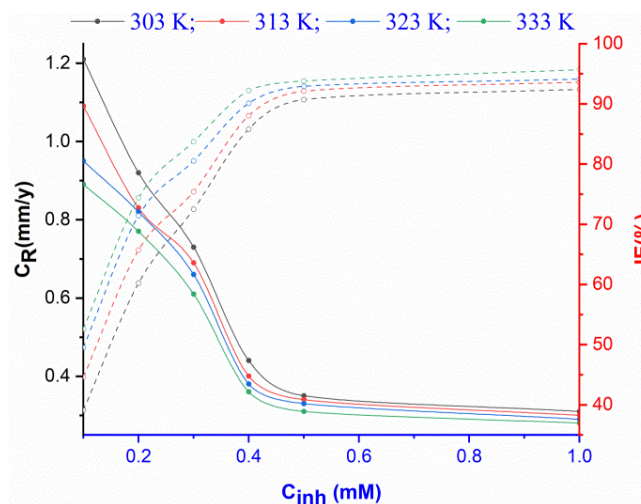
Figure 4. Variation in inhibitive efficiency on the surface of mild steel in 1 M HCl across different temperatures.
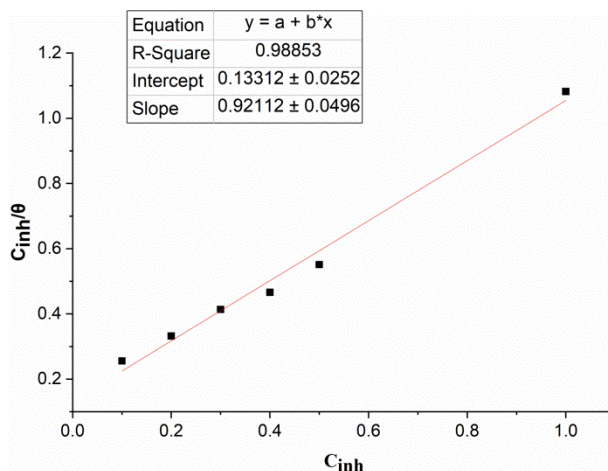
3.2. Adsorption Isotherm

The adsorption isotherm analysis provides insights into the interactions between inhibitor molecules and the metal surface, crucial for understanding corrosion inhibition mechanisms. In this study, surface coverage (θ) values were computed at various inhibitor concentrations in 1 M hydrochloric acid solution to elucidate these interactions. The two most commonly utilized adsorption isotherm models, Temkin and Langmuir, were employed for this purpose [41, 42]. Efforts to fit weight loss measurement data into different adsorption isotherms revealed that the Langmuir adsorption isotherm model best described the experimental data. According to the Langmuir model, the concentration of inhibitor in the corrosive solution (C_{inh}) is related to the degree of surface coverage (θ) by Equation 3 [40, 43]. The linear regression analysis between C_{inh}/θ and C_{inh} yielded an R^2 value of 0.988, as depicted in Figure 5. Figure 5 illustrates the linear relationship between C_{inh}/θ and C_{inh} at 303 K. These results confirm that the slope and R^2 value are both equal to 1, validating the adherence of PYB molecule adsorption on the mild steel surface to Langmuir isotherms. However, the deviation of the slope of the plot from unity suggests non-ideal behavior, which may arise from interactions among the adsorbed PYB molecules on the metal surface [44, 45].

Furthermore, the adsorption free energy (ΔG°_{ads}) and K_{ads} were determined using Equation 11:

$$\Delta G^{\circ}_{ads} = -RT \ln(55.5 K_{ads}) \tag{11}$$

where 55.5 represents the water concentration (mol/L), and R is the gas constant.

Equation	y = a + b*x
R-Square	0.98853
Intercept	0.13312 ± 0.0252
Slope	0.92112 ± 0.0496

Figure 5. Langmuir adsorption isotherm model for the adsorption of PYB in 1 M HCl on the surface of mild steel.

Typically, a ΔG^0_{ads} value of around -20 kJ/mol or lower is indicative of physisorption, while values around -40 kJ/mol or higher suggest chemisorption. In this study, the determined ΔG^0_{ads} value of -32.5 kJ/mol signifies a mechanism of adsorption involving both chemical and electrostatic interactions between PYB and mild steel in 1 M HCl solution at 303 K. The negative value of ΔG^0_{ads} indicates that the adsorption of inhibitor molecules onto the mild steel surface is a spontaneous process [46–51]. This comprehensive analysis sheds light on the complex nature of PYB's interaction with the metal surface, providing valuable insights into its corrosion inhibition mechanism in acidic environments.

3.3. Theoretical Calculation

Quantum chemical computations were conducted to evaluate the corrosion inhibition efficacy of the tested inhibitor molecules by analyzing their frontier molecular orbital (FMO) energy levels. This computational approach offers valuable insights into the protective performance of inhibitors, eliminating the need for extensive lab analyses and conserving time and resources [52]. In Table 2, various quantum chemical parameters essential for assessing the protection efficacy of the inhibitor molecules are presented. These parameters include the FMO energies (E_{HOMO} and E_{LUMO}), the energy gap between E_{HOMO} and E_{LUMO} (ΔE), dipole moment, global hardness (η), softness (σ), electronegativity (χ), and the fraction of electron transfer (ΔN). The E_{HOMO} signifies a molecule's capability to donate a lone pair of electrons, while the E_{LUMO} represents its tendency to accept electrons. The ΔE value, calculated as the energy difference between E_{HOMO} and E_{LUMO}, indicates the molecule's reactivity. A smaller ΔE value suggests higher reactivity, as seen in Table 2.

Table 2. Quantum chemical parameters for PYB molecule.

Parameter	Value
E_{HOMO} (eV)	−7.160
E_{LUMO} (eV)	1.452
ΔE (eV)	8.612
Dipole moment (Debye)	−7.8604
Global hardness (η)	4.306
Softness (σ)	0.232
Electronegativity (χ)	2.354
ΔN (Fraction of electron transfer)	0.951

Comparing with previously studied molecules, PYB exhibits the lowest ΔN value (2.608 eV), indicating its high reactivity. Additionally, the polarity of a molecule, indicated by its dipole moment, influences its corrosion inhibition efficacy. In this study, the dipole moment of PYB was found to be −7.8604 Debye, suggesting a considerable degree of polarity [53, 54]. Furthermore, the global hardness (η), softness (σ), and electronegativity (χ) offer insights into the dynamic parameters of the molecules. A higher ΔN value indicates enhanced inhibitory effectiveness, as demonstrated by Lukovit's research [55]. Equations 6 to 10 provide the mathematical expressions for calculating ΔE, η, σ, χ, and ΔN. These parameters collectively contribute to understanding the molecular interactions and reactivity, essential for predicting the corrosion inhibition efficacy of PYB and similar inhibitor molecules. Overall, the theoretical calculations offer a comprehensive understanding of the molecular characteristics and interactions underlying the corrosion inhibition mechanism, providing valuable guidance for the design and optimization of effective corrosion inhibitors. The optimized molecular structure of 2-Piperazin-1-yl-1,3-benzothiazole (PYB) provides insights into its spatial arrangement and geometry. This optimized structure represents the most stable conformation of PYB, obtained through quantum chemical calculations. The Highest Occupied Molecular Orbital (HOMO) structure reveals the distribution of electron density in PYB. Regions of high electron density, depicted in blue, indicate areas where electrons are most likely to be found. The HOMO structure illustrates the electron-donating capability of PYB, which is crucial for its interaction with metal surfaces. Conversely, the Lowest Unoccupied Molecular Orbital (LUMO) structure illustrates regions of low electron density, depicted in red [56–60]. These regions represent sites where electrons can be accepted, indicating PYB's potential to accept electrons from metal atoms. Understanding the distribution of electron density in the LUMO structure provides valuable insights into the reactivity and corrosion inhibition mechanism of PYB. The optimized molecular structure (Figure 6a) showcases the stable conformation of PYB, highlighting its three-dimensional arrangement. This optimized

structure serves as a basis for further analysis of PYB's chemical properties and interactions with metal surfaces. The HOMO structure (Figure 6b) indicates the electron-rich regions of PYB, emphasizing its ability to donate electrons. This electron-donating capability is essential for PYB's interaction with metal surfaces, where it can form coordination bonds and adsorb onto the surface, thereby inhibiting corrosion. Conversely, the LUMO structure (Figure 6c) reveals regions of low electron density, suggesting sites where PYB can accept electrons. This electron-accepting property enables PYB to interact with metal atoms, facilitating the formation of protective layers on the metal surface. Overall, the analysis of the optimized structure, HOMO, and LUMO structures provides valuable insights into the electronic properties and reactivity of PYB, contributing to a deeper understanding of its corrosion inhibition mechanism. These structural insights aid in the design and development of more effective corrosion inhibitors for industrial applications [61–63].

a　　　　　　　　　　　　　b　　　　　　　　　　　　　c
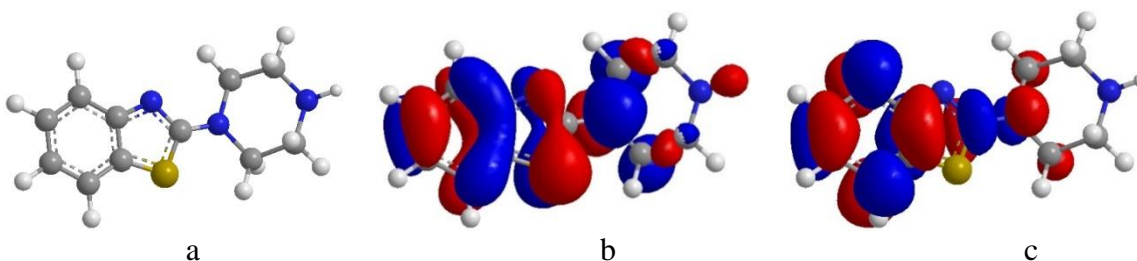
Figure 6. Structural Analysis of PYB.

3.4. Suggested inhibition mechanism

The inhibition mechanism of 2-piperazin-1-yl-1,3-benzothiazole (PYB) in hydrochloric acid (HCl) solution involves multiple steps, driven by the interaction between PYB molecules and the metal surface. Here is a suggested mechanism based on experimental observations and theoretical considerations [64–66]:

1. **Adsorption onto metal surface:** PYB molecules adsorb onto the mild steel surface through both physical and chemical interactions. The presence of nitrogen and sulfur atoms in the PYB structure facilitates coordination bonds with the metal surface, leading to the formation of a protective layer.
2. **Chemical interaction with metal:** The nitrogen and sulfur atoms in PYB molecules exhibit a high affinity for the d-orbitals of iron atoms on the metal surface. This results in the formation of coordination complexes, where PYB molecules act as Lewis bases, donating electron pairs to the metal ions, thereby reducing their reactivity.
3. **Formation of protective film:** As PYB molecules continue to adsorb onto the metal surface, they form a dense and stable protective film. This film acts as a barrier, preventing the corrosive species, such as HCl, from reaching the metal surface and initiating corrosion reactions.

4.**Electron transfer:** The presence of electron-donating heteroatoms in PYB facilitates electron transfer processes between the inhibitor molecules and the metal surface. This electron transfer leads to the reduction of metal ions, inhibiting their dissolution into the corrosive solution.

5.**Synergistic effects:** PYB molecules may also interact with other species present in the corrosive environment, such as chloride ions, enhancing the inhibition efficiency through synergistic effects. These interactions further stabilize the protective film and inhibit corrosion processes.

6.**Temperature dependency:** While the inhibition mechanism remains effective over a range of temperatures, variations in temperature can influence the rate of adsorption and the stability of the protective film. Higher temperatures may promote faster adsorption kinetics and strengthen the interactions between PYB molecules and the metal surface, thereby enhancing inhibition efficiency.

7.**Theoretical insights:** Quantum chemical calculations provide additional insights into the inhibition mechanism by revealing the electronic structure and reactivity of PYB molecules. The frontier molecular orbital (FMO) analysis indicates the ability of PYB to donate and accept electrons, supporting its role as an effective corrosion inhibitor.

In conclusion, the inhibition mechanism of PYB in HCl solution involves adsorption onto the metal surface, formation of a protective film, electron transfer processes, and synergistic effects with other species. The proposed mechanism highlights the multifaceted nature of corrosion inhibition and underscores the importance of understanding molecular interactions for the design of effective inhibitors.

The inhibition of mild steel corrosion in 1 M hydrochloric acid by PYB occurs primarily through an adsorption process, although the exact mechanism involves a complex interplay of physical and chemical interactions. Understanding this mechanism is crucial for elucidating how PYB effectively mitigates corrosion rates. In the case of PYB, it is conceivable that inhibitor molecules adhere to the mild steel surface primarily *via* van der Waals forces, representing a physical adsorption process. This formation of a protective layer acts as a barrier between the metal substrate and the corrosive acid, thereby diminishing the corrosion rate. Furthermore, PYB exhibits the capacity for chemical reactivity with corrosion byproducts present on the metal surface, further attenuating corrosion rates. For example, PYB may engage in reactions with iron oxides formed on the steel surface, yielding a protective film that impedes further corrosion progression. The adsorption process of PYB onto the mild steel surface in 1 M hydrochloric acid is intricate, involving both physical and chemical interactions. Figure 7 illustrates various mechanisms that elucidate the adsorption process [67–70].

1.Protonated PYB molecules or ions exist within the corrosive medium. Through electrostatic attraction, these ions are deposited onto the mild steel interface where Cl^- ions had previously been adsorbed (physical adsorption).

2. PYB can undergo chemical adsorption onto the metallic surface by donating lone pairs of electrons from nitrogen and sulfur atoms to vacant orbitals of iron atoms.

3. π-Electrons from benzene and heterocyclic rings, along with the unoccupied d-orbitals of iron atoms, engage in electron donation and acceptance interactions [71–72].
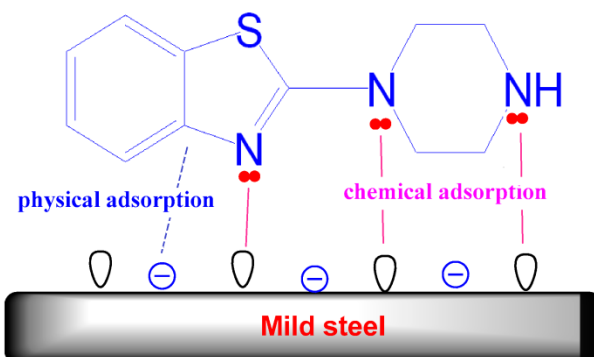
Figure 7. Proposed inhibition mechanism of PYB as a corrosion inhibitor.

In summary, the inhibition mechanism of PYB involves a combination of physical adsorption *via* van der Waals forces and chemical interactions with the metal surface and corrosion products. This multifaceted approach effectively reduces corrosion rates, offering valuable insights into the protective action of PYB against mild steel corrosion in acidic environments.

Conclusion

The findings presented in this study offer valuable insights into the corrosion inhibition potential of 2-piperazin-1-yl-1,3-benzothiazole (PYB) for mild steel in 1 M hydrochloric acid solution. Through a comprehensive investigation encompassing the impact of inhibitor concentration, immersion periods, and temperature, we have demonstrated the efficacy of PYB in mitigating corrosion and protecting mild steel surfaces. Our results indicate that increasing the concentration of PYB leads to a significant reduction in the corrosion rate of mild steel, with optimal inhibition efficiency observed at higher concentrations. Furthermore, we observed that extending the immersion period enhances the protective properties of PYB, suggesting a time-dependent adsorption process that contributes to prolonged corrosion inhibition. Additionally, the influence of temperature on the corrosion inhibition process was elucidated, revealing that higher temperatures facilitate enhanced inhibitor adsorption and formation of a protective layer on the metal surface, thereby further reducing the corrosion rate. This underscores the importance of considering temperature variations in corrosion inhibition studies.

While this study primarily relies on weight-loss measurements to assess corrosion rates, the mechanistic insights gained from our findings provide a solid foundation for further exploration using complementary experimental techniques such as electrochemical measurements and surface analysis methods. Future research could delve deeper into

understanding the molecular interactions between PYB and mild steel surfaces, as well as elucidating the role of temperature and solution conditions in corrosion inhibition processes. Overall, our study contributes to the broader field of corrosion inhibition by offering a comprehensive evaluation of PYB as a potential corrosion inhibitor for mild steel in acidic environments. The insights gained from this research pave the way for the development of more effective corrosion inhibitors and provide valuable guidance for mitigating corrosion in industrial applications.

References

1. B.S. Mahdi, M.K. Abbass, M.K. Mohsin, W.K. Al-Azzawi, M.M. Hanoon, M.H.H. AlKaabi, L.M. Shaker, A.A. Al-Amiery, W.N.R.W. Isahak, A.A.H. Kadhum and M.S. Takriff, Corrosion inhibition of mild steel in hydrochloric acid environment using terephthaldehyde based on Schiff base: Gravimetric, thermodynamic, and computational studies, *Molecules*, 2022, **27**, 4857. doi: 10.3390/molecules27154857

2. Q.A. Jawad, D.S. Zinad, R.D. Salim, A.A. Al-Amiery, T.S. Gaaz, M.S. Takriff and A. Kadhum, Synthesis, Characterization, and Corrosion Inhibition Potential of Novel Thiosemicarbazone on Mild Steel in Sulfuric Acid Environment, *Coatings*, 2019, **9**, 729. doi: 10.3390/coatings9110729

3. S.B. Al-Baghdadi, F.T.M. Noori, W.K. Ahmed and A.A. Al-Amiery, Thiadiazole as a potential corrosion inhibitor for mild steel in 1 M HCl, *J. Adv. Electrochem.*, 2016, **2**, 67–69.

4. A.M. Resen, M. Hanoon, R.D. Salim, A.A. Al-Amiery, L.M. Shaker and A.A.H. Kadhum, Gravimetrical, theoretical, and surface morphological investigations of corrosion inhibition effect of 4-(benzoimidazole-2-yl) pyridine on mild steel in hydrochloric acid, *Koroze Ochr. Mater.*, 2020, **64**, 122–130. doi: 10.2478/kom2020-0018

5. A.Y.I. Rubaye, M.T. Mohamed, M.A.I. Al-Hamid, A.M. Mustafa, F.F. Sayyid, M.M. Hanoon, A.H. Kadhum, A.A. Alamiery and W.K. Al-Azzawi, Evaluating the corrosion inhibition efficiency of 5-(4-pyridyl)-3-mercapto-1,2,4-triazole for mild steel in HCl: insights from weight loss measurements and DFT calculations, *Int. J. Corros. Scale Inhib.*, 2024, **13**, no. 1, 185–222. doi: 10.17675/2305-6894-2024-13-1-10

6. N. Muneam, F.F. Sayyid, M.H.H. Al-Kaabi and A.A. Alamiery, Environmentally friendly synthesis and characterization of copper nanoparticles using amino acids as capping agents: enhanced corrosion resistance and morphological control, *Int. J. Corros. Scale Inhib.*, 2024, **13**, no. 1, 288–310. doi: 10.17675/2305-6894-2024-13-1-14

7. Mohammed, H.S. Aljibori, M.A.I. Al-Hamid, W.K. Al-Azzawi, A.A.H. Kadhum and A. Alamiery, N-Phenyl-N′-[5-phenyl-1,2,4-thiadiazol-3-yl]thiourea: corrosion inhibition of mild steel in 1 M HCl, *Int. J. Corros. Scale Inhib.*, 2024, **13**, no. 1, 38–78. doi: 10.17675/2305-6894-2024-13-1-3

8. W.K. Al-Azzawi, A.J. Al Adily, F.F. Sayyid, R.K. Al-Azzawi, M.H. Kzar, H.N. Jawoosh, A.A. Al-Amiery, A.A.H. Kadhum, W.N.R.W. Isahak and M.S. Takriff,

Evaluation of corrosion inhibition characteristics of an N-propionanilide derivative for mild steel in 1 M HCl: Gravimetrical and computational studies, *Int. J. Corros. Scale Inhib.*, 2022, **11**, no. 3, 1100–1114. doi: [10.17675/2305-6894-2022-11-3-12](10.17675/2305-6894-2022-11-3-12)

9. A.M. Mustafa, F.F. Sayyid, N. Betti, M.M. Hanoon, A. Al-Amiery, A.A.H. Kadhum and M. Takriff, Inhibition Evaluation of 5-(4-(1H-pyrrol-1-yl)phenyl)-2-mercapto-1,3,4-oxadiazole for the Corrosion of Mild Steel in an Acid environment: Thermodynamic and DFT Aspects, *Tribologia*, 2021, **38**, 39–47. doi: [10.30678/fjt.105330](10.30678/fjt.105330)

10. A.M. Mustafa, F.F. Sayyid, N. Betti, L.M. Shaker, M.M. Hanoon, A.A. Alamiery, A.A.H. Kadhum and M.S. Takriff, Inhibition of mild steel corrosion in hydrochloric acid environment by 1-amino-2-mercapto-5-(4-(pyrrol-1-yl)phenyl)-1,3,4-triazole, *S. Afr. J. Chem. Eng.*, 2022, **39**, 42–51. doi: 10.1016/j.sajce.2021.11.009

11. M. Rezaeivala, S. Karimi, K. Sayin and B. Tüzün, Experimental and theoretical investigation of corrosion inhibition effect of two piperazine-based ligands on carbon steel in acidic media, *Colloids Surf.*, *A*, 2022, **641**, 128538. doi: 10.1016/j.colsurfa.2022.128538

12. Sheetal, S. Sengupta, M. Singh, S. Thakur, B. Pani, P. Banerjee, S. Kaya and A. Singh, An insight about the interaction of Aryl Benzothiazoles with mild steel surface in aqueous HCl solution, *J. Mol. Liq.*, 2022, **354**, 118890. doi: 10.1016/j.molliq.2022.118890

13. A.M. Resen, M.M. Hanoon, W.K. Alani, A. Kadhim, A.A. Mohammed, T.S. Gaaz, A.A.H. Kadhum, A.A. Al-Amiery and M.S. Takriff, Exploration of 8-piperazine-1-ylmethylumbelliferone for application as a corrosion inhibitor for mild steel in hydrochloric acid solution, *Int. J. Corros. Scale Inhib.*, 2021, **10**, no.1, 368–387. doi: [10.17675/2305-6894-2021-10-1-21](10.17675/2305-6894-2021-10-1-21)

14. D.K. Verma, M. Kazi, M.S. Alqahtani, R. Syed, E. Berdimurodov, S. Kaya, R. Salim, A. Asatkar and R. Haldhar, N-hydroxybenzothioamide derivatives as green and efficient corrosion inhibitors for mild steel: Experimental, DFT and MC simulation approach, *J. Mol. Struct.*, 2021, **1241**, 130648. doi: 10.1016/j.molstruc.2021.130648

15. P. Kumari G. Anusha, J. Mishma, R. Sinha, A. Suvarna and S. Gaonkar, New benzisoxazole derivative: A potential corrosion inhibitor for mild steel in 0.5 M hydrochloric acid medium-insights from electrochemical and density functional theory studies, *Heliyon*, 2023, **9**, e21014.

16. R. Sheetal, R.A. Singh, M. Singh, S. Thakur, B. Pani and S. Kaya, Advancement of corrosion inhibitor system through N-heterocyclic compounds: a review, *Corros. Eng.*, *Sci. Technol.*, 2023, **58**, 73–101. doi: [10.1080/1478422X.2022.213797](10.1080/1478422X.2022.213797)

17. *Standard Practice for Preparing, Cleaning, and Evaluating Corrosion Test*, ASTM International, 2011, 1–9.

18. G.R. Monama, M.J. Hato, K.E. Ramohlola, T.C. Maponya, S.B. Mdluli, K.M. Molapo, K.D. Modibane, E.I. Iwuoha, K. Makgopa and M.D. Teffu, Hierarchiral 4-tetranitro copper (II) phthalocyanine based metal organic framework hybrid

composite with improved electrocatalytic efficiency towards hydrogen evolution reaction, *Results Phys*., 2019, **15**, 102564. doi: 10.1016/j.rinp.2019.102564

19. A.S. Fouda, M.A. Ismail, A.S. Abousalem and G.Y. Elewady, Experimental and theoretical studies on corrosion inhibition of 4-amidinophenyl-2,2'-bifuran and its analogues in acidic media, *RSC Adv*., 2017, **7**, 46414–46430. doi: 10.1039/C7RA08092A

20. A.J.M. Eltmimi, A. Alamiery, A.J. Allami, R.M. Yusop, A.H. Kadhum and T. Allami, Inhibitive effects of a novel efficient Schiff base on mild steel in hydrochloric acid environment, *Int. J. Corros. Scale Inhib*., 2021, **10**, 634–648. doi: 10.17675/2305-6894-2021-10-2-10

21. R. Zhang, H. Yang, Y. Sun, W. Song, X. Zhu, Ya. Wang, Y. Wang, Y.C. Pan and Z. Zhang, Competitive Adsorption of 4-Methyl-4H-1,2,4-triazole-3-thiol and Na Salt of Phytic Acid on a Silver Surface: Raman Spectral and Electrochemical Observations, *J. Phys. Chem. C*, 2009, **113**, 9748–9754. doi: 10.1021/jp900329s

22. M.J. Frisch, G.W. Trucks, H.B. Schlegel, G.E. Scuseria, M.A. Robb, J.R. Cheeseman, J.A. Montgomery, Jr. T. Vreven, K.N. Kudin, J.C. Burant, J.M. Millam, S.S. Iyengar, J. Tomasi, V. Barone, B. Mennucci, M. Cossi, G. Scalmani, N. Rega, G.A. Petersson, H. Nakatsuji, M. Hada, M. Ehara, K. Toyota, R. Fukuda, J. Hasegawa, M. Ishida, T. Nakajima, Y. Honda, O. Kitao, H. Nakai, M. Klene, X. Li, J.E. Knox, H.P. Hratchian, J.B. Cross, V. Bakken, C. Adamo, J. Jaramillo, R. Gomperts, R.E. Stratmann, O. Yazyev, A.J. Austin, R. Cammi, C. Pomelli, J.W. Ochterski, P.Y. Ayala, K. Morokuma, G.A. Voth, P. Salvador, J.J. Dannenberg, V.G. Zakrzewski, S. Dapprich, A.D. Daniels, M.C. Strain, O. Farkas, D.K. Malick, A.D. Rabuck, K. Raghavachari, J.B. Foresman, J.V. Ortiz, Q. Cui, A.G. Baboul, S. Clifford, J. Cioslowski, B.B. Stefanov, G. Liu, A. Liashenko, P. Piskorz, I. Komaromi, R.L. Martin, D.J. Fox, T. Keith, M.A. Al-Laham, C.Y. Peng, A. Nanayakkara, M. Challacombe, P.M.W. Gill, B. Johnson, W. Chen, M.W. Wong, C. Gonzalez and J.A. Pople, *Gaussian 03, Revision B. 05*, Gaussian, Wallingford, CT, 2004.

23. T. Koopmans, Ordering of wave functions and eigen-energies to the individual electrons of an atom, *Physica*, 1934, 1, 104–113. doi: 10.1016/S0031-8914(34)90011-2

24. A.L. Jembere and M.B. Genet, Effect of low calcination temperature on the corrosion inhibition performance of biomass based Na_2SiO_3 on mild steel immersed in tap water, *Cogent Engineering*, 2023, **10**, 2165631. doi: 10.1080/23311916.2023.2165631

25. S.H. Alrefaee, K.Y. Rhee, C. Verma, M.A. Quraishi and E.E. Ebenso, Challenges and advantages of using plant extract as inhibitors in modern corrosion inhibition systems: Recent advancements, *J. Mol. Liq*., 2021, **321**, 114666. doi: 10.1016/j.molliq.2020.114666

26. R. Haldhar, D. Prasad, I. Bahadur, O. Dagdag and A. Berisha, Evaluation of Gloriosa superba seeds extract as corrosion inhibition forlow carbon steel in sulfuric acidic medium: A combined experimentaland computational studies, *J. Mol. Liq*., 2021, **323**, 114958. doi: 10.1016/j.molliq.2020.114958

27. P. Muthukrishnan, B. Jeyaprabha and P. Prakash, Adsorption and corrosion inhibiting behavior of Lannea coromandelica leaf extract on mild steel corrosion, *Arabian J. Chem*., 2017, **10**, S2343–S2354. doi: 10.1016/j.arabjc.2013.08.011

28. A.R. Hoseizadeh, I. Danaee and M.H. Maddahy, Thermodynamic and adsorption behaviour of vitamin B1 as a corrosion inhibitor for AISI 4130 steel alloy in HCl solution, *Zeitschrift für Physikalische Chemie*, 2013, **227**, 403–418. 10.1524/zpch.2013.0276

29. B. Hammouti, A. Zarrouk, S.S. Al-Deyab and I. Warad, Temperature Effect, Activation Energies and Thermodynamics of Adsorption of ethyl 2-(4-(2-ethoxy-2-oxoethyl)-2- pTolylquinoxalin-1(4H)-yl) Acetate on Cu in HNO3, *Orient. J. Chem*., 2011, **27**, 23–31.

30. Z. Amjad, R.T. Landgraf and J.L. Penn, Calcium sulfate dihydrate (gypsum) scale inhibition by PAA, PAPEMP, and PAA/PAPEMP blend, *Int. J. Corros. Scale Inhib*., 2014, **3**, no. 1, 35–47. doi: 10.17675/2305-6894-2014-3-1-035-047

31. J.C. Valle-Quitana, G.F. Dominguez-Patiño and J.G. Gonzalez-Rodriguez, Corrosion Inhibition of Carbon Steel in 0.5 M H₂SO₄ by Phthalocyanine blue, *Int. Scholarly Res. Not*., 2014, **2014**, 945645. doi: 10.1155/2014/945645

32. P. Zhao, Q. Liang and Y. Li, Electrochemical, SEM/EDS and quantum chemical study of phthalocyanines as corrosion inhibitors for mild steel in 1 mol/L HCl, *Appl. Surf. Sci*., 2005, **252**, 1596–1607. doi: 10.1016/j.apsusc.2005.02.121

33. K. Sakamoto and E. Ohno-Okumura, Syntheses and functional properties of phthalocyanines, *Materials*, 2009, **2**, 1127–1179. doi: 10.3390/ma2031127

34. G. De La Torre, P. Vazquez, F. Agullo-Lopez and T. Torres, Role of structural factors in the nonlinear optical properties of phthalocyanines and related compounds, *Chem. Rev*., 2004, **104**, 3723–3750. doi: 10.1021/cr030206t

35. M.A. García-Sánchez, F. Rojas-González, E.C. Menchaca-Campos, S.R. Tello-Solís, R. Quiroz-Segoviano, L.A. Diaz-Alejo, E. Salas-Bañales and A. Campero, Crossed and linked histories of tetrapyrrolic macrocycles and their use for engineering pores within sol-gel matrices, *Molecules*, 2013, **18**, 588–653. doi: 10.3390/molecules18010588

36. L.O. Olasunkanmi, I.B. Obot, M.M. Kabanda and E.E. Ebenso, Some quinoxalin-6-yl derivatives as corrosion inhibitors for mild steel in hydrochloric acid: Experimental and theoretical studies, *J. Phys. Chem. C*, 2015, **119**, 16004–16019. doi: 10.1021/acs.jpcc.5b03285

37. T. Pesha, G.R. Monama, M.J. Hato, T.C. Maponya, M.E. Makhatha, K.E. Ramohlola, K.M. Molapo, K.D. Modibane and M.S. Thomas, Inhibition Effect of Phthalocyaninatocopper (II) and 4-Tetranitro (phthalocyaninato) copper (II) Inhibitors for Protection of Aluminum in Acidic Media, *Int. J. Electrochem. Sci*., 2019, **14**, 137–149. doi: 10.20964/2019.01.17

38. M. Dibetsoe, L.O. Olasunkanmi, O.E. Fayemi, S. Yesudass, B. Ramaganthan, I. Bahadur, A.S. Adekunle, M.M. Kabanda and E.E. Ebenso, Some phthalocyanine and naphthalocyanine derivatives as corrosion inhibitors for aluminum in acidic medium:

Experimental, quantum chemical calculations, QSAR studies and synergistic effect of iodide ions, *Molecules*, 2015, **20**, 15701–15734. doi: 10.3390/molecules200915701

39. J. Xu, Y. Wang and Z. Zhang, Potential and concentration dependent electrochemical dealloying of Al2Au in sodium chloride solutions, *J. Phys. Chem. C*, 2012, **116**, 5689–5699. doi: 10.1021/jp210488t

40. S.K. Shukla and E.E. Ebenso, Corrosion Inhibition, Adsorption Behavior and Thermodynamic Properties of Streptomycin on Mild Steel in Hydrochloric Acid Medium, *Int. J. Electrochem. Sci.*, 2011, **6**, 3277–3291. doi: 10.1016/S1452-3981(23)18251-4

41. I. Langmuir, The constitution and fundamental properties of solid and liquids. II. Liquids, *J. Am. Chem. Soc.*, 1917, **39**, 1848–1906. doi: 10.1021/ja02254a006

42. M. Lagrenée, B. Mernari, M. Bouanis, M. Traisnel and F. Bentiss, Study of the mechanism and inhibiting efficiency of 3,5-bis(4-methylthiophenyl)-4H-1,2,4-triazole on mild steel corrosion in acidic media, *Corros. Sci.*, 2002, **44**, 573–588. doi: 10.1016/S0010-938X(01)00075-0

43. I.D. Mall, V.C. Srivastava, N.K. Agrwal and I.M. Mishra, Adsorptive removal of malachite green dye from aqueous solution by bagasse fly ash and activated carbonkinetic study and equilibrium isotherm analysis, *Colloids Surf.*, A, 2005, **264**, 17–28. doi: 10.1016/j.colsurfa.2005.03.027

44. E.A. Noor and A.H. Al-Moubaraki, Thermodynamic study of metal corrosion and inhibitor adsorption processes in mild steel/1-methyl-4[4'-(-X)-styryl pyridinium iodides/hydrochloric acid systems, *Mater. Chem. Phys.*, 2008, **110**, 145–154. doi: 10.1016/j.matchemphys.2008.01.028

45. S.K. Sharma, A. Peter and I.B. Obot, Potential of Azadirachta indica as a green corrosion inhibitor against mild steel, aluminum, and tin: a review, *J. Anal. Sci. Technol.*, 2015, **6**, 26. doi: 10.1186/s40543-015-0067-0

46. P. Udhayakala, T.V. Rajendirin and S. Gunasekaran, Theoretical Evaluation of Corrosion Inhibition Performance of Some Triazole Derivatives, *J. Adv. Sci. Res.*, 2012, **3**, 71–77.

47. S.O. Adejo and M.M. Ekwenchi, Proposing a new empirical adsorption isotherm known as Adejo-Ekwenchi isotherm, *IOSR J. Appl. Chem.*, 2014, 6, 66–71.

48. A.A. Siaka, N.O. Eddy, S.O. Idris, A. Muhammad, C.M. Elinge and F.A. Atiku, *Innovations Sci. Eng.*, 2012, **2**, 41.

49. M. Lebrini, F. Robert and C. Ross, Inhibition Effect of Alkaloids Extract from Annona Squamosa Plant on the Corrosion of C38 Steel in Normal Hydrochloric Acid Medium, *Int. J. Electrochem. Sci.*, 2010, **5**, 1698–1712. doi: 10.1016/S1452-3981(23)15422-8

50. Y.S. Ho, J.F. Porter and G. McKay, Water, Air, *Soil Pollut.*, 2000, **141**, 1.

51. A. Popova, M. Christov, A. Vasilev and A. Zwetanova, Mono- and dicationic benzothiazolic quaternary ammonium bromides as mild steel corrosion inhibitors. Part I: Gravimetric and voltammetric results, *Corros. Sci.*, 2011, **53**, 679–686. doi: 10.1016/j.corsci.2010.10.005

52. S. Hadisaputra, A.A. Purwoko, I. Ilhamsyah, S. Hamdiani, D. Suhendra, N. Nuryono and B. Bundjali, A combined experimental and theoretical study of (E)-ethyl 3-(4-methoxyphenyl) acrylate as corrosion inhibitor of iron in 1 M HCl solutions, *Int. J. Corros. Scale Inhib.*, 2018, **7**, 633–647. doi: [10.17675/2305-6894-2018-7-4-10](https://doi.org/10.17675/2305-6894-2018-7-4-10)

53. S. Hadisaputra, A.A. Purwoko, Rahmawati, D. Asnawati, I.S. Hamdiani and Nuryono, Experimental and Theoretical Studies of (2R)-5-hydroxy-7-methoxy-2-phenyl-2,3-dihydrochromen-4-one as corrosion inhibitor for Iron in Hydrochloric Acid, *Int. J. Electrochem. Sci.*, 2019, **14**, 11110–11121. doi: [10.20964/2019.12.77](https://doi.org/10.20964/2019.12.77)

54. S. Hadisaputra, A.A. Purwoko, A. Hakim, R. Wati, D. Asnawati and Y.P. Prananto, Experimental and Theoretical Study of Pinostrobin as Copper Corrosion Inhibitor at 1 M H_2SO_4 Medium, *IOP Conf. Ser.: Mater. Sci. Eng.*, 2020, **833**, 012010. doi: [10.1088/1757-899X/833/1/012010](https://doi.org/10.1088/1757-899X/833/1/012010)

55. S. Hadisaputra, A.A. Purwoko, F. Wajdi, I. Sumarlan and S. Hamdiani, Theoretical study of the substituent effect on corrosion inhibition performance of benzimidazole and its derivatives, *Int. J. Corros. Scale Inhib.*, 2019, **8**, 673–688. doi: [10.17675/2305-6894-2019-8-3-15](https://doi.org/10.17675/2305-6894-2019-8-3-15)

56. V.S. Sastri and J.R. Perumareddi, Molecular orbital theoretical studies of some organic corrosion inhibitors, *Corrosion*, 1997, **53**, 617–622. doi: [10.5006/1.329029476](https://doi.org/10.5006/1.329029476)

57. S. Hadisaputra, Z. Iskandar and D. Asnawati, Prediction of the Corrosion Inhibition Efficiency of Imidazole Derivatives: A Quantum Chemical Study, *Acta Chim. Asiana*, 2019, **2**, 88–94. doi: [10.29303/aca.v2i1.15](https://doi.org/10.29303/aca.v2i1.15)

58. N.O. Eddy, S.R. Stoyanov and E.E. Ebenso, Fluoroquinolones as corrosion inhibitors for mild steel in acidic medium; experimental and theoretical studies, *Int. J. Electrochem. Sci.*, 2010, **5**, 1127–1150. doi: [10.1016/S1452-3981(23)15350-8](https://doi.org/10.1016/S1452-3981(23)15350-8)

59. Y. Wirayani, M. Ulfa and Y. Yahmin, Corrosion inhibition efficiency of nicotine based on quantum chemical study, *Acta Chim. Asiana*, 2018, **1**, 37–42. doi: [10.29303/aca.v1i2.29](https://doi.org/10.29303/aca.v1i2.29)

60. A.S. Fouda, M.A. Ismail, A.S. Abousalem and G.Y. Elewady, Experimental and theoretical studies on corrosion inhibition of 4-amidinophenyl-2,2′-bifuran and its analogues in acidic media, *RSC Adv.*, 2017, **7**, 46414–46430. doi: [10.1039/C7RA08092A](https://doi.org/10.1039/C7RA08092A)

61. M. Stern and A.L. Geary, Electrochemical polarization, I. A theoretical analysis of the shape of polarisation curves, *J. Electrochem. Soc.*, 1957, **104**, 56–63. doi: [10.1149/1.2428496](https://doi.org/10.1149/1.2428496)

62. M.A. Amin, M.A. Ahmed, H.A. Arida, F. Kandemirli, M. Saracoglu, T. Arslan and M.A. Basaran, Monitoring corrosion and corrosion control of iron in HCl by non-ionic surfactants of the TRITON-X series–part III. Immersion time effects and theoretical studies, *Corros. Sci.*, 2011, **53**, 1895–1909. doi: [10.1016/j.corsci.2011.02.007](https://doi.org/10.1016/j.corsci.2011.02.007)

63. K.F. Khaled and M.M. Al-Qahtani, The Inhibitive effect of some tetrazole derivatives towards Al corrosion in acid solution: chemical, electrochemical and theoretical studies, *Mater. Chem. Phys.*, 2009, **113**, 150–158. doi: 10.1016/j.matchemphys.2008.07.060

64. D.B. Hmamou, R. Salghi, A. Zarrouk, H. Zarrok, R. Touzani, B. Hammouti and A. El Assyry, Investigation of corrosion inhibition of carbon steel in 0.5 M H$_2$SO$_4$ by new bipyrazole derivative using experimental and theoretical approaches, *J. Environ. Chem. Eng.*, 2015, **3**, 2031–2041. doi: 10.1016/j.jece.2015.03.018

65. H. Ma, S. Chen, Z. Liu and Y. Sun, Theoretical elucidation on the inhibition mechanism of pyridine-pyrazole compound: a Hartree Fock study, *J. Mol. Struct.: THEOCHEM*, 2006, **774**, 19–22. doi: 10.1016/j.theochem.2006.06.044

66. B.D.B. Tiu and R.C. Advincula, Polymeric Corrosion Inhibitors for the Oil and Gas Industry: Design Principles and Mechanism, *React. Funct. Polym.*, 2015, **95**, 25–45. doi: 10.1016/j.reactfunctpolym.2015.08.006

67. M. Lagrenée, B. Mernari, M. Bouanis, M. Traisnel and F. Bentiss, Study of the mechanism and inhibiting efficiency of 3,5-bis(4-methylthiophenyl)-4H-1,2,4-triazole on mild steel corrosion in acidic media, *Corros. Sci.*, 2002, **44**, 573–588. doi: 10.1016/S0010-938X(01)00075-0

68. H.M. Luaibi, N. Betti, S.S. Al-Taweel, T.S. Gaaz and A.A. Alamiery, Inhibition mechanism and corrosion protection of mild steel in HCl using coumarin derivative: Gravimetrical and theoretical analysis, *Int. J. Corros. Scale Inhib.*, 2024, **13**, no. 2, 1056–1083. doi: 10.17675/2305-6894-2024-13-2-23

69. O.E. Chyhyrynets, Y.F. Fateev, V.I. Vorobiova and M.I. Skyba, Study of the Mechanism of Action of the Isopropanol Extract of Rapeseed Oil Cake on the Atmospheric Corrosion of Copper, *Mater. Sci.*, 2016, **51**, 644–651. doi: 10.1007/s11003-016-9886-4

70. M.A.I. Al-Hamid, S.B. Al-Baghdadi, T.S. Gaaz, A.A. Khadom, E. Yousif and A. Alamiery, Green chemistry solutions: Harnessing pharmaceuticals as environmentally friendly corrosion inhibitors: A review, *Int. J. Corros. Scale Inhib.*, 2024, **13**, 630–670. doi: 10.17675/2305-6894-2024-13-2-1

71. A. Shaban, I. Felhosi and J. Telegdi, Laboratory assessment of inhibition efficiency and mechanism of inhibitor blend (P22SU) on mild steel corrosion in high chloride containing water, *Int. J. Corros. Scale Inhib.*, 2017, **6**, 262–275. doi: 10.17675/2305-6894-2017-6-3-3

72. A. Mohammed, H.S. Aljibori, M.A.I. Al-Hamid, W.K. Al-Azzawi, A.A.H. Kadhum and A. Alamiery, N-Phenyl-N′-[5-phenyl-1,2,4-thiadiazol-3-yl]thiourea: corrosion inhibition of mild steel in 1 M HCl, *Int. J. Corros. Scale Inhib.*, 2024, **13**, 38–78. doi: 10.17675/2305-6894-2024-13-1-3

◆ ◆ ◆